4th International Conference on Structural Health Monitoring of Intelligent Infrastructure (SHMII-4) 2009
22-24 July 2009, Zurich, Switzerland

Sub-Pixel Edge Detection for Structural Health Monitoring

Laurence Pap, Ju Jia Zou, Brian Uy and Yang Xiang

School of Engineering,
University of Western Sydney,
Locked Bag 1797 Penrith South DC NSW 1797 Australia

ABSTRACT: In structural engineering it is essential to monitor the health of structural members under various load conditions. Traditionally, engineers are required to travel on site to retrieve various test results. However, in modern times, engineers can remotely monitor test results both statistically and visually with the help of image processing. When image processing is applied to structural health monitoring, one major problem to overcome is the offset of an actual edge location caused by the digitalization of straight lines. It is important to locate the edges of objects as accurately as possible to ensure that correct data is received and correct decisions are made. This paper presents a new edge detection algorithm at the sub-pixel level for the purpose of structural health monitoring. By using sub-pixel edge detection, we can achieve higher precision than other methods, which are limited by the resolution of imaging devices. Non-linear image interpolation is used to increase the precision of determining edges by estimating values which are at undefined points. By using non-linear interpolation, the over smoothing effect produced by linear methods can be overcome. The proposed method, when applied to structural health monitoring, can perform a more accurate and efficient determination of the edges of an object than previous edge detection methods. The proposed method also benefits in images, that are noisy compared to previous edge detection methods. Experiment results on sample objects show the superiority of the proposed method.

1 INTRODUCTION

Each year, a vast amount of money and resources are invested in the development of structural infrastructures. However, the monitoring of the behavior of these structures is often overlooked and as the aging process occurs, problems develop for engineers in latter years due to the engineers being unprepared to deal with these problems. In the early 1990s, structural health monitoring was started to determine and predict the integrity and condition of structural objects. Traditional structural health monitoring involves identifying damage using different sensor technologies such as accelerometers, strain gages, extensometers, fiber optic sensors and thermocouples. Due to the diversity of these classical techniques, structural engineers are faced with many challenges as a wide range of expertise is needed to obtain a sufficient amount of data to determine the health of structural objects.

In recent years, optical measurement techniques have been developed to overcome the complexities of traditional approaches and also to remotely monitor structural objects in real time (Lecompte et al. (2006), Mass et al. (2006)). These techniques are efficient and accurate

in measurements for structural health monitoring. However they require expensive photogrammetric equipment which are limited by the resolution of those devices. With the development of faster and more cost-effective computers and processors which are widely available today, image processing has become popular due to its abilities to overcome the physical limitation of photogrammetric equipment through software.

When image processing is applied to structural health monitoring it is important to locate the edges and boundaries of an object as accurately as possible to ensure that correct data is received and correct decisions are made. This can be achieved by applying an edge detection algorithm on the image produced by the imaging device. An edge detection algorithm functions by detecting edges which are defined in digital images as two adjacent points where a strong intensity change occurs. There have been a number of different edge detection algorithms that have been developed such as Prewitt, Sobel and Canny and are widely accepted and used (Canny (1986)). However, one major problem to overcome is the offset of an actual edge location caused by the digitalization of straight lines. These offsets therefore diminish the accuracy of the edge detection algorithms and incorrect locations of the edges may result. This is particularly true for applications where fine edges and accurate locations of an object are required for purposes for structural health monitoring. Therefore to solve this critical problem, sub-pixel edge detection techniques can be preformed on the digital images.

There have been many different techniques developed to estimate the sub-pixel edge positions, these include a method which locates discontinuities in images by using a zero crossing detector (Binford et al. (1981)), methods which use spatial or Zernike moments of an edge using edge operators (Overington et al. (1986), Lyvers et al. (1989)), a method which uses an analogue-based approach from the first derivative of an output from a CCD image for a fast sub-pixel level edge detection (Ohtani et al. (2001)), a method which uses a Zernike moment combined with Sobel operators to find a sub-pixel approximation to improve accuracy (Qu et al. (2004)) and methods which use image interpolation techniques obtained from a polynomial to estimate a sub-pixel edge approximation (Kubota et al. (2001), Xie et al. (2005)). Image interpolation techniques provide an accurate sub-pixel approximation by estimating values which are at undefined points. These techniques are particularly useful in low resolution images and structural health monitoring where cost-effective photogrammetric equipment can be purchased to produce similar accuracy to photogrammetric equipment which are expensive.

Interpolation techniques can be divided into two types, linear and non-linear interpolation. Both bilinear interpolation and cubic convolution use a linear approach where a polynomial is evaluated with the same stencil for every pixel in the image. This provides a low computation time for the interpolation. However, it ignores the local features of an image and an over smoothing effect is produced near the discontinuities in the digital image.

Non-linear interpolation methods have been development to overcome the problems introduced by linear methods however they require more computation time for processing. Non-linear interpolation methods based on wave-lets have been developed to impose no continuity constraints in the interpolation to sharpen edges and to avoid over smoothing near the discontinuities (Carey et al. (1999)). Another popular non-linear method called the Essentially Non-Oscillatory (ENO) interpolation was originally developed to overcome the problem of smoothing across discontinuities in fluid dynamics applications and then was later modified for sub-pixel image processing applications (Harten et al. (1987), Balaguer et al. (2001)). The ENO interpolation method selects a stencil for a polynomial calculation based on the grey-level intensity variation of a pixel and its surrounding pixels. This is done by computing a standard Newton divided difference of the pixels in the image to form a measure of their smoothness. Two contiguous sets of points are then formed using the divided differences. The contiguous set of points with the lower divided differences is added to stencil.

A modification of the ENO interpolation method, namely the Geometric Shock-Capturing ENO method (GENO) was developed to further enhance discontinuities and to locate curves with higher sub-pixel accuracy then ENO (Siddiqi et al. (1995)). Another recent modification of the ENO method uses a 4th order interpolation ENO method to achieve a finer grid of pixels to increase the geometric accuracy for edge detection (Hermosilla et al. (2008)). This method considers the pixels of an image as either point values or cell averages of a function for the purpose of improving the localization and geometry of the edges at a sub-pixel level. The method also applies a gradient based edge detection to attain sub-pixel edge detection.

These methods provide good localization and good detection where edges are marked relatively close to the real edges of an image. For the application of structural health monitoring, it is important to locate the edges of a real object as accurately as possible to ensure that correct data is received and correct decisions are made. In practice, noise is also an issue due to the limitation and imperfection of imaging devices and therefore affects the ability of these algorithms to achieve accurate results.

This paper presents a new edge detection algorithm at the sub-pixel level for the purpose of structural health monitoring. The proposed method is based upon the ENO interpolation method and follows the scheme introduced by Hermosilla et al. The proposed method also integrates the canny edge detector with the ENO interpolation scheme to provide a more accurate and efficient determination of the edges of an object than previous edge detectors. The proposed method also aims to increase the accuracy in images that contain noise.

The paper is organized as follows. In Section 2 the proposed interpolation and edge detection algorithm is described. Section 3 presents the experimental results to illustrate the superiority of the proposed method when compared to previous edge detection methods and finally concluding remarks are given in Section 4.

2 METHODOLOGY

The proposed method is based upon the ENO interpolation method however unlike previous methods, which apply a gradient based edge detector after interpolation, the proposed method combines a 4th order ENO interpolation method with the Canny edge detector. When an object is digitalized, it is represented by a set of pixels which are used to form a two dimensional image matrix. The proposed method considers that the pixels of an image represent the grey level cell average function $\overline{\overline{g}}_{i,j}$ according to Harten (1989) and Hermosilla et al. (2008):

$$\overline{\overline{g}}_{i,j} = \frac{1}{h^2}\int_{y_j-\frac{h}{2}}^{y_j+\frac{h}{2}} \int_{x_i-\frac{h}{2}}^{x_i+\frac{h}{2}} g(x,y)dxdy, \tag{1}$$

Where $g(x,y)$ is the discrete grey level value of an image, x and y are the coordinates of a pixel, i and j are the coordinates of a cell and h is the size of a cell.

The first step of the proposed method is to increase the resolution of the pixels in the image. This is done by dividing a cell average into four new sub cell averages $\overline{\overline{g}}_{i,j}^{(n)}$ where $n \in \{1,2,3,4\}$. This can be computed according to the procedure described in the paper written by Hermosilla et al. (2008). Figure 1 illustrates the new resolution obtained from dividing the cell averages into four new sub cell averages.

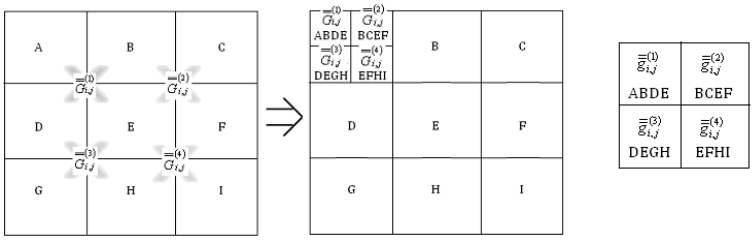

Figure 1. The process of dividing a cell average into four new sub cell averages

The second step of the proposed method is to remove noise from the new sub cell averages. This is done in order to prevent noise from being interpolated because it can cause false readings of the edges of an object. A mean convolution filter is applied to the cell average values to smooth the edges of the image and to remove noise. The filtered output $\overline{\overline{G}}_{i,j}$ can be found by the convolution defined as:

$$\overline{\overline{G}}_{i,j} = \sum_{l=-N/2}^{N/2} \sum_{m=-M/2}^{M/2} K(x,y)\overline{\overline{g}}_{i,j}(x-l, y-m) \quad \text{where } K(x,y) = \begin{bmatrix} \frac{1}{9} & \frac{1}{9} & \frac{1}{9} \\ \frac{1}{9} & \frac{1}{9} & \frac{1}{9} \\ \frac{1}{9} & \frac{1}{9} & \frac{1}{9} \end{bmatrix} \tag{2}$$

represents the kernel of size $N \times M$ and $\overline{\overline{g}}_{i,j}$ is the input image containing the cell averages.

The third step of the proposed method is to perform a sub-pixel estimation using the filtered cell averages $\overline{\overline{G}}_{i,j}$ and a 4th order ENO interpolation. Given that $p_{i,j}\left(x_*; \overline{\overline{G}}\right)$ is a unique one-dimensional third-degree polynomial where x_* is the sub-pixel approximation in the x horizontal direction and because we only have the discrete filtered cell average values $\overline{\overline{G}}_{i,j}$, we interpolate $\overline{\overline{G}}_{i,j}(x)$ by $p_{i,j}\left(x_*; \overline{\overline{G}}\right)$ in order to approximate the sub-pixel filtered cell average values (Harten et al. (1987)). The procedure is described as followed:

Let $\overline{\overline{G}}_{k\min,j}$ be a filtered cell average value at point $k_{\min,j}$ where k is the horizontal coordinate of a pixel, j is the vertical coordinate of a pixel and the subscript min denotes the first horizontal coordinate in the stencil. The ENO interpolation stencil $\left\{\overline{\overline{G}}_{k\min,j}, \overline{\overline{G}}_{k\min,j}+1, \overline{\overline{G}}_{k\min,j}+2, \overline{\overline{G}}_{k\min,j}+3\right\}$ is formed from four successive points in the x horizontal direction using the filtered cell averages. This stencil is repeated for all the data sets in the x horizontal direction.

Assuming that the following initial conditions $k^{(0)}_{\min,j} = k$, $p^{(0)}_{i,j}\left(x_*; \overline{\overline{G}}\right) = \overline{\overline{G}}_{i,j}$ are considered, the standard Newton divided differences can be computed according to Harten et al. (1987) as:

$$a^{(m)}_{i.j} = \overline{\overline{G}}_{i,j}\left[x_{k^{(m-1)}_{\min,j}}, ..., x_{k^{(m-1)}_{\min,j}}+m\right]\Big|_{y=j} \qquad b^{(m)}_{i.j} = \overline{\overline{G}}_{i,j}\left[x_{k^{(m-1)}_{\min,j}}-1, .., x_{k^{(m-1)}_{\min,j}}+m-1\right]\Big|_{y=j}, \tag{3}$$

where m denotes the order. The ENO stencil selection and the divided difference equation have been modified to include the discrete filtered cell averages $\overline{\overline{G}}_{i,j}(x)$ as shown in Equation 3. This allows for a larger set of data points for the interpolation due to the increased resolution found in the filtered cell averages. Following the method of a standard ENO interpolation, the possible points with the lower divided difference are then added to the stencil to form a sub-pixel approximation:

$$p^{(m)}_{i,j}\left(x_*; \overline{\overline{G}}\right) = p^{(m-1)}_{i,j}(x_*; \overline{\overline{G}}) + c^{(m)}_{i,j} \prod_{i=k^{(m-1)}_{\min,j}}^{k^{(m-1)}_{\min,j}+m-1} (x_* - x_i) \tag{4}$$

Where $c_{i.j}^{(m)}$ is either $b_{i.j}^{(m)}$ if $a_{i.j}^{(m)} \geq b_{i.j}^{(m)}$ or $a_{i.j}^{(m)}$ otherwise. $p_{i,j}^{(m)}\left(x_*;\overline{\overline{G}}\right)$ gives the sub-pixel approximation values for the x horizontal direction.

Using the set of sub-pixel approximated values calculated in Equation 4, the ENO procedure is then repeated for values in the y vertical direction. The ENO interpolation stencil $\left\{\overline{\overline{G}}_{j\min,x_*}, \overline{\overline{G}}_{j\min,x_*}+1, \overline{\overline{G}}_{j\min,x_*}+2, \overline{\overline{G}}_{j\min,x_*}+3\right\}$ is formed from four successive points in the y vertical direction. The following initial conditions $j_{\min,x_*}^{(0)} = j$ and $q_{j,x_*}^{(0)}\left(y_*;p\right) = p_{j,x_*}$ are considered where $q_{j,x_*}\left(y_*;p\right)$ is a unique one-dimensional third-degree polynomial according to Harten et al. (1987) and y_* is the sub-pixel approximation in the y horizontal direction. The standard Newton divided differences can be computed according to Harten et al. (1987) as:

$$a_{j.x_*}^{(m)} = p_{j,x_*}\left[y_{l_{\min,x_*}^{(m-1)}},...,y_{l_{\min,x_*}^{(m-1)}}+m\right]\Big|_{y=x_*} \qquad b_{j.x_*}^{(m)} = p_{j,x_*}\left[y_{l_{\min,x_*}^{(m-1)}}-1,...,y_{l_{\min,x_*}^{(m-1)}}+m-1\right]\Big|_{y=x_*} \tag{5}$$

Following the method of a standard ENO interpolation, the possible points with the lower divided difference are then added to the stencil to form a sub-pixel approximation:

$$q_{j,x_*}^{(m)}\left(y_*;p\right) = q_{j,x_*}^{(m-1)}\left(y_*;p\right) + c_{j,x_*}^{(m)} \prod_{j=l_{\min,x_*}^{(m-1)}}^{l_{\min,x_*}^{(m-1)}+m-1}\left(y_* - y_j\right) \tag{6}$$

Where $c_{j.x_*}^{(m)}$ is either $b_{j.x_*}^{(m)}$ if $a_{j.x_*}^{(m)} \geq b_{j.x_*}^{(m)}$ or $a_{j.x_*}^{(m)}$ otherwise. $q_{j,x_*}^{(m)}\left(y_*;p\right)$ gives the sub-pixel approximation values for the y vertical direction. The sub-pixel approximations from Equation 4 and Equation 6 are combined to form $R\left(x_*,y_*;\overline{\overline{G}}\right)$ which is the sub-pixel estimation values for the interpolated image.

The fourth step of the proposed method is to perform a modification of the Canny Edge detector (Canny (1986)). The calculated sub-pixel approximations are used during the non-maximum suppression stage of the Canny edge detector to suppress non-maximum values which are not considered to be an edge, to 0. This involves finding the local maximum values which occur at a peak in the gradient function:

$$LocalMax = \begin{cases} \max\left[R\left(x_*-1,y_*;\overline{\overline{G}}\right), R\left(x_*+1,y_*;\overline{\overline{G}}\right)\right] & if \quad \theta = 0° \\ \max\left[R\left(x_*-1,y_*+1;\overline{\overline{G}}\right), R\left(x_*+1,y_*-1;\overline{\overline{G}}\right)\right] & if \quad \theta = 45° \\ \max\left[R\left(x_*,y_*+1;\overline{\overline{G}}\right), R\left(x_*,y_*-1;\overline{\overline{G}}\right)\right] & if \quad \theta = 90° \\ \max\left[R\left(x_*+1,y+1_*;\overline{\overline{G}}\right), R\left(x_*-1,y_*-1;\overline{\overline{G}}\right)\right] & if \quad \theta = 135° \end{cases}, \tag{7}$$

Where θ represent the orientation of an edge. Sub-pixel approximation values which are equal to or larger than the local maximum are considered not to be edges and are suppressed to 0:

$$O\left(x_*,y_*;\overline{\overline{G}}\right) = \begin{cases} R\left(x_*,y_*;\overline{\overline{g}}\right) & if \quad R\left(x_*,y_*;\overline{\overline{g}}\right) < LocalMax \\ 0 & otherwise \end{cases}, \tag{8}$$

where $O\left(x_*,y_*;\overline{\overline{G}}\right)$ denotes the output image. Therefore, $R\left(x_*,y_*;\overline{\overline{G}}\right)$ gives the sub-pixel estimation values for the interpolated image and $O\left(x_*,y_*;\overline{\overline{G}}\right)$ gives the coordinates of the edge points at the sub-pixel level.

3 EXPERIMENTAL RESULTS

The proposed method was tested using various synthetic images and is evaluated against previous method to show its superiority. In image processing, an ideal reference image is non-existent due to the discretization of real values when an object is digitalized. However, synthetic images with known geometry shapes can be used to compare the accuracy of edge detection methods to the theoretical calculated edges of a known geometry shape. Figure 2 illustrates the experimental results of the proposed method when compared to the Canny edge detector with no sub-pixel estimation and with a 4th order interpolation based on cell averages (Canny (1986), Hermosilla et al. (2008)). It can be seen that the detected edges in the proposed method are better defined and less staggered then the previous two methods. Table 1 illustrates the calculated root mean squared error of the estimated edge locations from each method using the circle synthetic image. It can be seen that the 4th order ENO method with Canny edge detection provides a vast improvement over Canny without any interpolation. This is due to the sub-pixel estimations in the interpolation process. It can also be seen that the best results are achieved by the proposed method. The computational time for each method is also recorded. The experimental results were preformed on an Intel Core 2 Quad CPU at 2.4GHz with 2 GB or ram and using the C# programming environment. It can be seen that both the proposed method and the 4th order ENO method are slower then Canny' method. However, they provide a more accurate result. The proposed method is slightly faster than the 4th order ENO method and this due to its integration into Canny.

Table 1. Analytical results for a circle synthetic image.

Method	Accuracy (Root mean squared error)	Computational Time (Seconds)
Canny (Canny (1986))	1.59	0.016
4th Order ENO Canny (Hermosilla et al. (2008))	0.60	2.203
Proposed Method	0.48	2.140

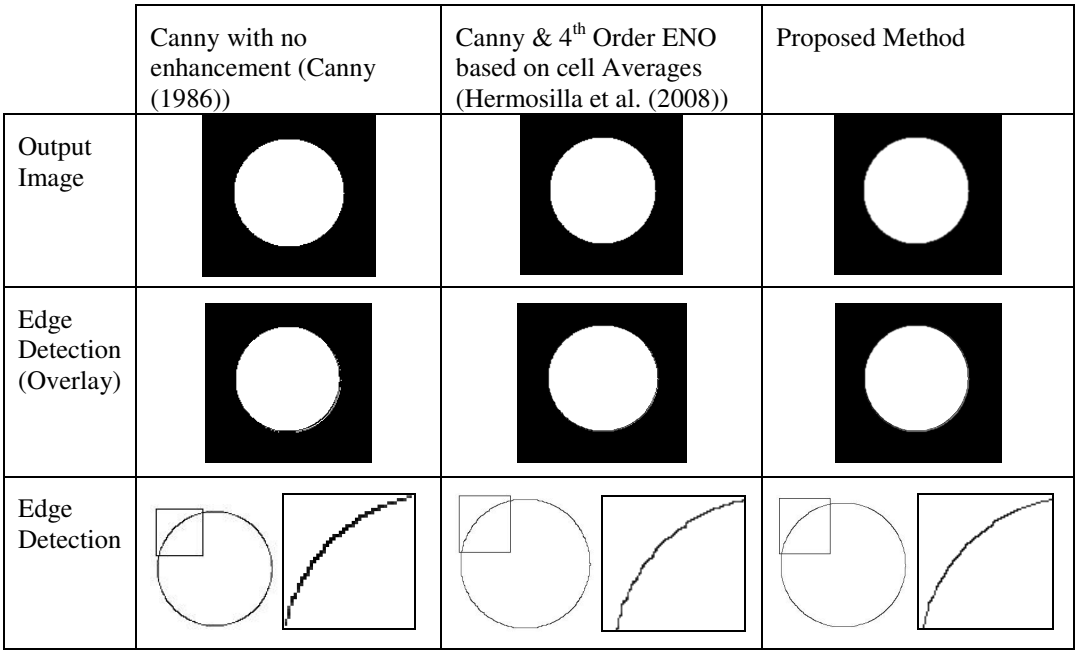

Figure 2. Experimental results of a circle synthetic image.

Figure 3 illustrates the experimental results for a circle synthetic image with Gaussian noise. Noise is of particular interest because in digital photogrammetric equipment and in particular cost effective equipment, noise is always introduced as the sensitivity of the image sensor is increased. It is important to remove noise from the image as it can cause false readings of the edges of an object. The same filter that is used in the proposed method is also applied to the noisy original image before Canny and 4th order ENO are applied. It can be seen in Figure 3 that both Canny and 4th Order ENO are affected by noise. Table 2 also illustrates the problem of noise and its significance on the accuracy of edge detection. It can be seen that the 4th order ENO method is affected by noise more than Canny without any sub-pixel estimation and this is due to the sub-pixel estimation of the noise in the interpolation process. It can be concluded that the best results are achieved by the proposed method and this is due to the integration of the mean filter in the interpolation process. The computational time for the proposed method is also slightly faster than the 4th order ENO method.

Table 2. Analytical results for a circle synthetic image with noise.

Method	Accuracy (Root mean squared error)	Computational Time (Seconds)
Canny (Canny (1986))	1.62	0.14
4th Order ENO Canny (Hermosilla et al. (2008))	2.82	3.270
Proposed Method	0.50	3.086

	Canny with no enhancement (Canny (1986))	Canny & 4th Order ENO based on cell Averages (Hermosilla et al. (2008))	Proposed Method
Output Image	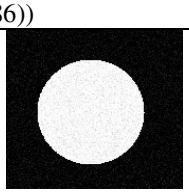		
Edge Detection (Overlay)			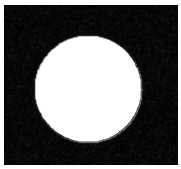
Edge Detection	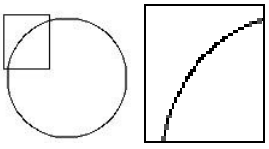	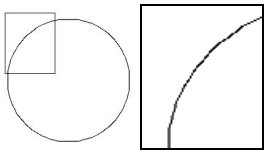	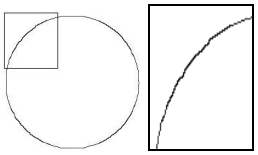

Figure 3. Experimental results of a circle synthetic image with noise.

4 CONCLUSION

This paper presents a new edge detection algorithm at the sub-pixel level for the purpose of structural health monitoring. By using sub-pixel edge detection, a higher precision than other methods, which are limited by the resolution of imaging devices, is achieved. The proposed method, when applied to structural health monitoring, can perform a more accurate and efficient determination of the edges of an object than previous edge detection methods.

The proposed method is based upon the ENO interpolation method and follows the scheme introduced by Hermosilla et al (2008). The proposed method also integrates the Canny edge detector with the ENO interpolation scheme. A mean convolution filter is introduced in this method to increase the accuracy in images that contain noise. As a result, the proposed method provides an effective and efficient determination of the edges of an object when compared to previous methods and especially on images that contain noise as shown in the experimental results.

REFERENCES

Balaguer, A, Conde, C, López and Marti´nez, V. 2001. A finite volume method with a modified ENO scheme using a Hermite interpolation to solve advection diffusion equations. International Journal on Numerical Methods in Engineering, 50: 2339-2371.

Binford, PJ and MacVicar-Whelan, PJ. 1981. Line finding with subpixel precision. *Proceeding of the Society of Photo-Optical Instrumentation Engineers,* 281: 26-31

Canny, J. 1986. A computation approach to edge detection. *IEEE Transaction on Pattern Analysis and Machine Intelligence,* 8: 679-698.

Carey, WK, Chuang, DB and Hemami, SS. 1999. Regularity-preserving image interpolation. *IEEE Transaction on Image* Processing, 8: 1293-1297.

Harten, A, Engquist, B, Osher, S and Chakravarthy, SR. 1987. Uniformly high order accurate essentially non-oscillatory schemes, III. Journal of Computational Physics, 71: 231-303.

Harten, A. 1987. ENO Schemes with Subcell Resolution. Journal of Computation Physics, 89: 148-184.

Hermosilla, T, Bermejo, E, Balaguer, A and Ruiz, LA. 2008. Non-linear fourth-order image interpolation for subpixel edge detection and localization, *Image and Vision Computing*, 26: 1240-1248.

Kubota, T, Huntsberger, T and Martin, JT. 2001. Edge based probabilistic relaxation for sub-pixel contour extraction, *Energy Minimization Methods in Computer Vision and Pattern Recognition, France,* 3: 328-348.

Lecomptem, D, Vantomme, J and Sol, H. 2006. Crack Detection in a Concrete Beam using two Different Camera Techniques, SAGE Publications, 5(1): 59-68.

Lyvers, EP, Mitchell, OR, Akey, ML and Reeves, AP. 1989. Subpixel measurements using a moment-based edge operator. *IEEE Transaction on Pattern Analysis and Machine Intelligence*, 11: 1293-1309.

Maas, H and Hampel, U. 2006. Photogrammetric Techniques in Civil Engineering Material Testing and Structural Monitoring. Photogrammetric Engineering & Remote Sensing, 72(1): 1-7.

Ohtani, K, and Baba, M. 2001. A Fast Edge Location Measurement with Subpixel Accuracy using a CCD Image. *IEEE Transaction on Instrumentation and Measurement Technology*, 18(3): 2087-2092

Overington, I and Greenway, P. 1987. Practical first-difference edge detection with subpixel accuracy. *Image and Vision Computing,* 5: 217-224.

Qu, YD, Cui, CS, Chen, SB and Li, Q. 2004. A fast subpixel edge detection method using Sobel-Zernike moments operate. *Image and Vision Computing,* 23: 11-17.

Siddiqi, K, Kimia, BB and Chu, C. 1995. Geometric Shock-Capturing ENO Schemes for Subpixel Interpolation, Computation, and Curve Evolution. *IEEE Transaction on Graphical Models and Image Processing*, 59(5): 437-442.

Xie, SH, Liao, Q and Qin, SR. 2005. Sub-pixel edge detection for precision measurement based on Canny criteria. *Key Engineering Materials,* 295-296: 711-716.